QUARTERLY OF APPLIED MATHEMATICS

VOLUME LVI SEPTEMBER · 1998 NUMBER 3

SEPTEMBER 1998, PAGES 401–412

EFFECTS DUE TO SHEAR FLOW ON THE DIFFUSIVE-THERMAL INSTABILITY OF PREMIXED GAS FLAMES

By

Y. KORTSARTS (*School of Mathematical Sciences, Tel-Aviv University, Israel*),

I. KLIAKHANDLER (*School of Mathematical Sciences, Tel-Aviv University, Israel*),

L. SHTILMAN (*School of Engineering, Tel-Aviv University, Israel*),

AND

G. I. SIVASHINSKY (*School of Mathematical Sciences, Tel-Aviv University, Israel and The Levich Institute for Physico-Chemical Hydrodynamics, City College of New York*)

Abstract. The diffusively unstable premixed gas flame is shown to be strongly affected by the background shear flow tangent to the flame interface. The pertinent flame-flow interaction alters both the flame stability limits and the character of its nonlinear evolution. The shear flow may expand the limits of the flame's diffusive instability simultaneously inducing new nonlinear saturation and linear dispersion effects similar to those occurring in KdV systems.

1. Introduction. Since the classical work of Taylor (1953) it is known that the unidirectional shear flow may markedly enhance the effective diffusivity of the soluble matter in the streamwise direction. It is therefore interesting to examine how this fundamental effect may manifest itself in the intrinsic dynamics of premixed gas flames, which are known to be highly sensitive to the interplay between thermal and molecular diffusivities of the system (e.g., Sivashinsky, 1990). To make the pertinent flame-flow interaction problem as simple as possible it is desirable to find a geometrical situation in which the undisturbed flame is unaffected by the shear flow. The flow enters the play only when the flame is disturbed. To meet such a requirement one may, for instance, consider a planar flame moving through a unidirectional shear flow parallel to the flame interface. Here the planar flame does not sense the underlying shear flow, which may be rather complex. However, being disturbed, the flame structure will immediately experience the impact of Taylor diffusivity, which may markedly influence the character of the flame evolution. Technically, the system is most tractable when the shear flow is completely

Received July 12, 1994.
1991 *Mathematics Subject Classification.* Primary 08A25.

©1998 Brown University

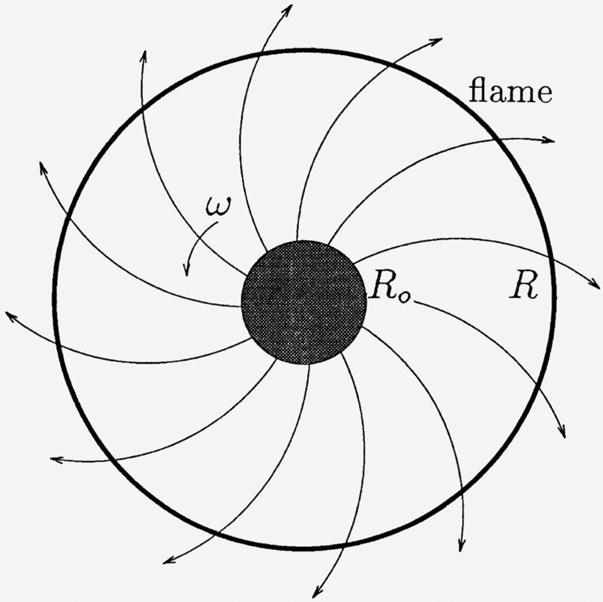

FIG. 1. Diagram depicting an unperturbed cylindrical flame stabilized on a rotating porous burner

time-independent in the frame of reference attached to the undisturbed flame. Such a situation occurs, for example, in a premixed flame stabilized on a porous cylindrical burner rotating about its axis of symmetry. Neglecting the density variation, this flame-flow system appears as is shown in Fig. 1. In polar coordinates $(\hat{r}, \varphi)$ the pertinent flow-field $(\hat{v}_r, \hat{v}_\varphi)$ reads:[1]

$$\hat{v}_r = \hat{Q}/(2\pi\hat{r}), \qquad \hat{v}_\varphi = \hat{R}_0^2\hat{\Omega}/\hat{r}. \tag{1.1}$$

Here $\hat{R}_0$, $\hat{\Omega}$, and $\hat{Q}$ are the porous burner radius, the burner rotation rate, and the total flow intensity, correspondingly.

The flow-field (1.1) obviously may sustain a steady cylindrical flame whose interface is located at

$$\hat{r} = \hat{R} = \hat{Q}/(2\pi\hat{U}_b) \tag{1.2}$$

where $\hat{U}_b$ is the burning velocity of the planar flame. The burner rotation clearly does not affect the circular equilibrium (1.2). Yet, it induces the shear

$$\frac{d\hat{v}_\varphi(\hat{R})}{d\hat{r}} = -\frac{\hat{R}_0^2\hat{\Omega}}{\hat{R}^2} = -\hat{a}, \tag{1.3}$$

which, as will be shown below, may significantly alter the flame stability.

[1] The subscript ^ labels the dimensional quantities.

2. Mathematical model. The stability of the cylindrical (circular) flame (Fig. 1) will be studied within the framework of a conventional constant-density near-equidiffusion model with suitably chosen nondimensional variables and parameters that reads (e.g., Matkowsky and Sivashinsky, 1979)

$$\frac{\partial \Theta}{\partial t} + v_r \frac{\partial \Theta}{\partial r} + \frac{v_\varphi}{r}\frac{\partial \Theta}{\partial \varphi} = \frac{\partial^2 \Theta}{\partial r^2} + \frac{1}{r}\frac{\partial \Theta}{\partial r} + \frac{1}{r^2}\frac{\partial^2 \Theta}{\partial \varphi^2}, \tag{2.1}$$

$$\frac{\partial S}{\partial t} + v_r \frac{\partial S}{\partial r} + \frac{v_\varphi}{r}\frac{\partial S}{\partial \varphi} = \frac{\partial^2 (S-\alpha\Theta)}{\partial r^2} + \frac{1}{r}\frac{\partial (S-\alpha\Theta)}{\partial r} + \frac{1}{r^2}\frac{\partial^2 (S-\alpha\Theta)}{\partial \varphi^2}. \tag{2.2}$$

Here

$$v_r = \frac{R}{r}, \qquad v_\varphi = \frac{aR^2}{r} \tag{2.3}$$

where $R = \hat{R}/\hat{l}_{\text{th}}$ is the nondimensional circular flame radius; $\hat{l}_{\text{th}} = \hat{D}_{\text{th}}/\hat{U}_b$ where $\hat{D}_{\text{th}}$ is the thermal diffusivity of the system; $R_0 = \hat{R}_0/\hat{l}_{\text{th}}$; $a = \hat{a}\hat{l}_{\text{th}}/\hat{U}_b$ is the nondimensional shear (1.3);

$$\Theta = \frac{\hat{T} - \hat{T}_0}{\hat{T}_b - \hat{T}_0}$$

is the reduced temperature of the system; $\hat{T}_0$ is the initial temperature of the fresh mixture; $\hat{T}_b$ is the adiabatic temperature of the burned gas;

$$S = \frac{(\hat{T}_b - \hat{T}_0)\hat{C} + (\hat{T} - \hat{T}_b)\hat{T}_a}{2\hat{C}_0\hat{T}_b^2}$$

is the reduced enthalpy, where $\hat{C}$ is the mass fraction of the deficient reactant; $\hat{C}_0$ is the initial level of mass fraction; $\hat{T}_a$ is the activation temperature of the chemical reaction ($\hat{T}_a \gg \hat{T}_b$); $r = \hat{r}/\hat{l}_{\text{th}}$, $t = \hat{t}\hat{U}_b/\hat{l}_{\text{th}}$, $\alpha = \hat{T}_a(\hat{T}_b - \hat{T}_0)(Le^{-1} - 1)/(2\hat{T}_b^2)$, where $Le = \hat{D}_{\text{th}}/\hat{D}_{\text{mol}}$ is the Lewis number (the ratio of thermal diffusivity to molecular diffusivity of the deficient reactant). The reaction zone is localized at the interface $r = \Phi(\varphi, t)$ where the following matching conditions hold:

$$\left[\frac{d\Theta}{dn}\right] + \exp S = 0, \tag{2.4}$$

$$\left[\frac{dS}{dn}\right] = \alpha\left[\frac{d\Theta}{dn}\right], \tag{2.5}$$

$$[\Theta] = 0, \qquad [S] = 0. \tag{2.6}$$

Here

$$\mathbf{n} = \frac{(1, -\Phi_\varphi/\Phi)}{\sqrt{1 + (\Phi_\varphi/\Phi)^2}}$$

is an outer normal to the flame interface $r = \Phi(\varphi, t)$.

In the burned gas, i.e., at $r > \Phi(\varphi, t)$,

$$\Theta(r, \varphi, t) \equiv 1. \tag{2.7}$$

The model (2.1)–(2.7) is a consistent asymptotics that may be formally derived from a pertinent reaction-diffusion-advection set of equations, provided $\hat{T}_a \gg \hat{T}_b$ (i.e., the activation temperature is high) and simultaneously $\alpha \sim (\hat{T}_a/\hat{T}_b)(Le^{-1} - 1)$ is a finite parameter (i.e., when $\hat{D}_{\mathrm{th}} \simeq \hat{D}_{\mathrm{mol}}$). At the entrance of the burner the temperature of the fresh mixture is $\hat{T}_0$ and the mass fraction of the deficient reactant is $\hat{C}_0$. Assuming that there is no heat-mass interaction between the burner skeleton and the flow, one may set

$$v_r \Theta = \frac{\partial \Theta}{\partial r}, \qquad v_r S = \frac{\partial (S - \alpha\Theta)}{\partial r} \quad \text{at } r = R_0. \tag{2.8}$$

For a steady cylindrical flame, i.e., when $\Phi = R$, the problem (2.1)–(2.8) yields the following basic solution:

$$\Theta^b = \left(\frac{r}{R}\right)^R \text{ at } r < R \quad \text{and} \quad \Theta^b = 1 \text{ at } r > R, \tag{2.9}$$

$$S^b = \alpha R \left(\frac{r}{R}\right)^R \ln\left(\frac{r}{R}\right) \text{ at } r < R \quad \text{and} \quad S^b = 0 \text{ at } r > R. \tag{2.10}$$

3. Asymptotic analysis. The nonlinear stability analysis will be carried out near $\alpha = 1$, the stability threshold of a freely propagating planar flame.[2] Henceforth, $\varepsilon = \alpha - 1$ will be employed as a parameter of expansion. In the absence of rotation, $\Omega = 0$, the related problem was discussed in Sivashinsky (1979). As has been shown in that study, in order to have a well-behaved asymptotics at $\varepsilon \to 0$ all the major variables and parameters of the system should be scaled as follows:

$$\begin{gathered} \Theta - \Theta^b = \varepsilon^2 \overline{\Theta}, \quad S - S^b = \varepsilon^2 \overline{S}, \quad \Phi - R = \varepsilon \overline{\Phi}, \quad \varphi = \varepsilon^{3/2} \bar{\varphi}, \\ t = \varepsilon^{-2} \bar{t}, \quad R = \varepsilon^{-2} \overline{R}, \quad R_0 = \varepsilon^{-2} \overline{R}_0, \quad \alpha = 1 + \varepsilon. \end{gathered} \tag{3.1}$$

As a result for the leading-order ε-approximation the following flame interface evolution equation was obtained:

$$\frac{\partial \overline{\Phi}}{\partial \bar{t}} + \frac{1}{2}\left(\frac{\partial \overline{\Phi}}{\partial \bar{x}}\right)^2 + \frac{\partial^2 \overline{\Phi}}{\partial \bar{x}^2} + 4\frac{\partial^4 \overline{\Phi}}{\partial \bar{x}^4} + \frac{\overline{\Phi}}{\overline{\overline{R}}} = 0 \quad (\bar{x} = \overline{R}\bar{\varphi}). \tag{3.2}$$

In the problem involving rotation, apart from the time scale associated with the instability induced growth rate, there emerges the second time scale conditioned by the drift of the large-scale disturbances. To avoid the cumbersome multiple-time asymptotic expansion it is helpful to pass from the original angular coordinate φ to the shifted one

$$\theta = \varphi - at \quad (a = \Omega R_0^2 / R^2) \tag{3.3}$$

where θ should be scaled as φ, i.e.,

$$\theta = \varepsilon^{3/2} \bar{\theta}. \tag{3.4}$$

[2]We mean here the instability leading to the formation of the so-called cellular flames occurring in low Lewis number premixtures. For high Lewis number systems one may well encounter a different, pulsating mode of instability. Despite rather scanty experimental data on the phenomenon in gaseous premixtures, in the combustion of some condensed mixtures, where $Le = \infty$, the pulsating instability appears to be quite feasible and received a good deal of attention both experimentally and theoretically (e.g., Bayliss and Matkowsky, 1990).

Apart from the drift the flame interface is also subject to the action of the shear (see (2.3))

$$\frac{dv_\varphi(R)}{dr} = -a \tag{3.5}$$

which is expected to augment the effective diffusivity of the system by a quantity of order $(dv_\varphi/dr)^2$, as happens in Taylor's problem. To make this impact comparable to that of negative diffusivity (see Eq. (3.2)) one should set

$$(dv_\varphi(R)/dr)^2 \sim \alpha - 1 = \varepsilon. \tag{3.6}$$

Hence, the shear should be scaled as

$$a = \varepsilon^{1/2}\bar{a}. \tag{3.7}$$

Rescaling the original problem (2.1)–(2.8) according to (3.1), (3.3), (3.4), (3.7) after a lengthy but otherwise straightforward algebra (see Appendix) one obtains

$$\frac{\partial\overline{\Phi}}{\partial\bar{t}} + \frac{1}{2}\left(\frac{\partial\overline{\Phi}}{\partial\bar{x}}\right)^2 - 2\bar{a}\overline{\Phi}\frac{\partial\overline{\Phi}}{\partial\bar{x}} + (1+40\bar{a}^2)\frac{\partial^2\overline{\Phi}}{\partial\bar{x}^2} - 20\bar{a}\frac{\partial^3\overline{\Phi}}{\partial\bar{x}^3} + 4\frac{\partial^4\overline{\Phi}}{\partial\bar{x}^4} + \frac{\overline{\Phi}}{\overline{R}} = 0 \quad (\bar{x} = \overline{R}\theta). \tag{3.8}$$

As is readily seen from the term $(1+40\bar{a}^2)\overline{\Phi}_{\bar{x}\bar{x}}$, the shear flow promotes the diffusive flame instability.[3] One should remember, however, that Eq. (3.8) is an approximation whose range of validity is restricted to the vicinity of $\alpha = 1$, the stability threshold of a freely propagating planar flame. Equation (3.2) and therefore Eq. (3.8) are not applicable for high Lewis number systems ($Le > 1, \alpha < 0$), where the shear flow is likely to exert an opposite, i.e., stabilizing influence. This issue, however, is out of the scope of this study and will be addressed in a future work.

Apart from affecting the stability threshold, the shear flame may generate travelling waves controlled by the dispersive term, $20\bar{a}\overline{\Phi}_{\bar{x}\bar{x}\bar{x}}$. The shear also produces a new quadratic nonlinearity $2\bar{a}\overline{\Phi}\,\overline{\Phi}_{\bar{x}}$, which emerges in numerous extended systems and, on par with the geometric term $\frac{1}{2}(\overline{\Phi}_{\bar{x}})^2$, is known to provide the nonlinear saturation of linearly unstable modes (e.g., Michelson and Sivashinsky, 1980). At $\bar{a} \ll 1$ the geometric nonlinearity clearly dominates over the shear one. However, at $\bar{a} \gg 1$, since $\bar{a}\bar{x} \sim 1$, both nonlinearities have a balanced impact on the system; none of them can be ignored. In the latter limit, Eq. (3.8) becomes

$$\Psi_\tau + \tfrac{1}{2}(\Psi_\xi)^2 - 2\Psi\Psi_\xi + 40\Psi_{\xi\xi} - 20\Psi_{\xi\xi\xi} + 4\Psi_{\xi\xi\xi\xi} + \gamma^{-1}\Psi = 0 \tag{3.9}$$

where

$$\Psi = \bar{a}^{-2}\overline{\Phi}, \qquad \xi = \bar{a}\bar{x}, \qquad \tau = \bar{a}^4\bar{t}, \qquad \gamma = \bar{a}^4\overline{R}.$$

[3]For example, a low Lewis number stable cylindrical flame may be destabilized by rotation of the burner.

The dispersion relation associated with Eq. (3.9) reads

$$\omega = (40k^2 - 4k^4) - \gamma^{-1} - 20ik^3 \quad (\Psi \sim \exp(\omega t + ik\xi)). \tag{3.10}$$

The instability sets in at $\gamma > \gamma_c = 1/100$ and $k_c = \sqrt{5}$, the wave number corresponding to the maximum growth rate of small harmonic perturbations.

4. Numerical simulations. In this section we present results of the numerical simulations of Eq. (3.9). The equation was solved over the interval $0 < \xi < 10\lambda_c$ subject to periodic boundary conditions ($\lambda_c = 2\pi k_c^{-1}$). The pseudo-spectral technique has been employed for the spatial discretization and the Adams' scheme for time advance. Since Eq. (3.9) has a strong damping in the high k range, all the scales were resolved at the

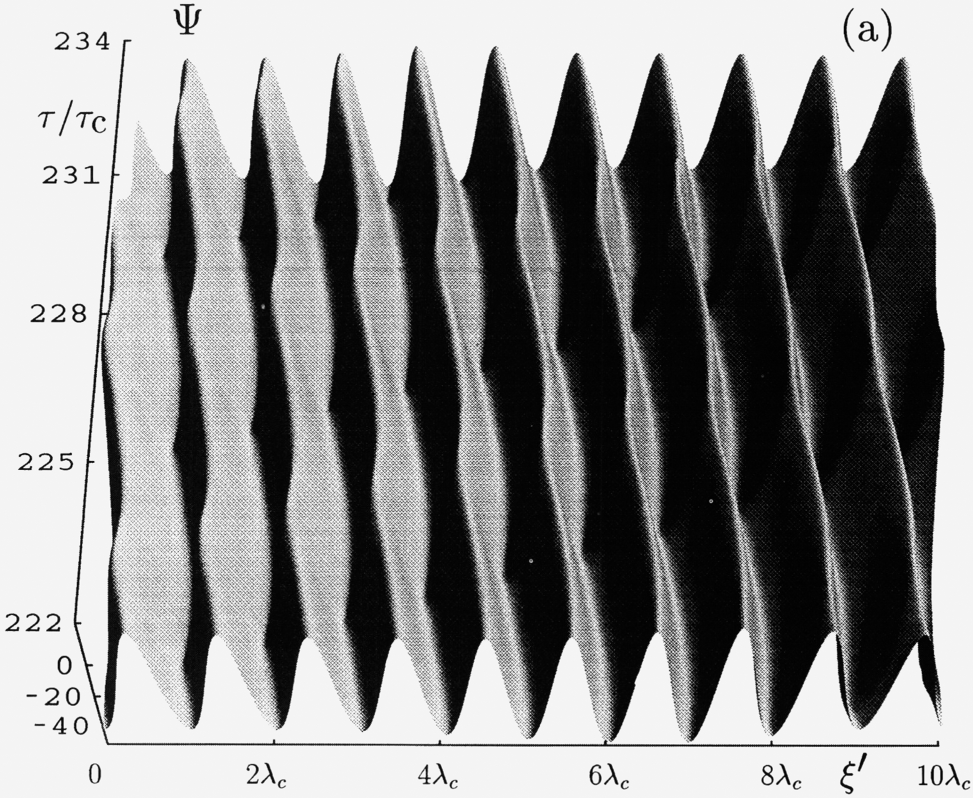

FIG. 2a. Numerical simulation of Eq. (3.9). $\langle\Psi\rangle$ versus time τ and $\xi' = \xi - V(\gamma)\tau$ for various values of γ ($0 < \xi' < 10\lambda_c$).

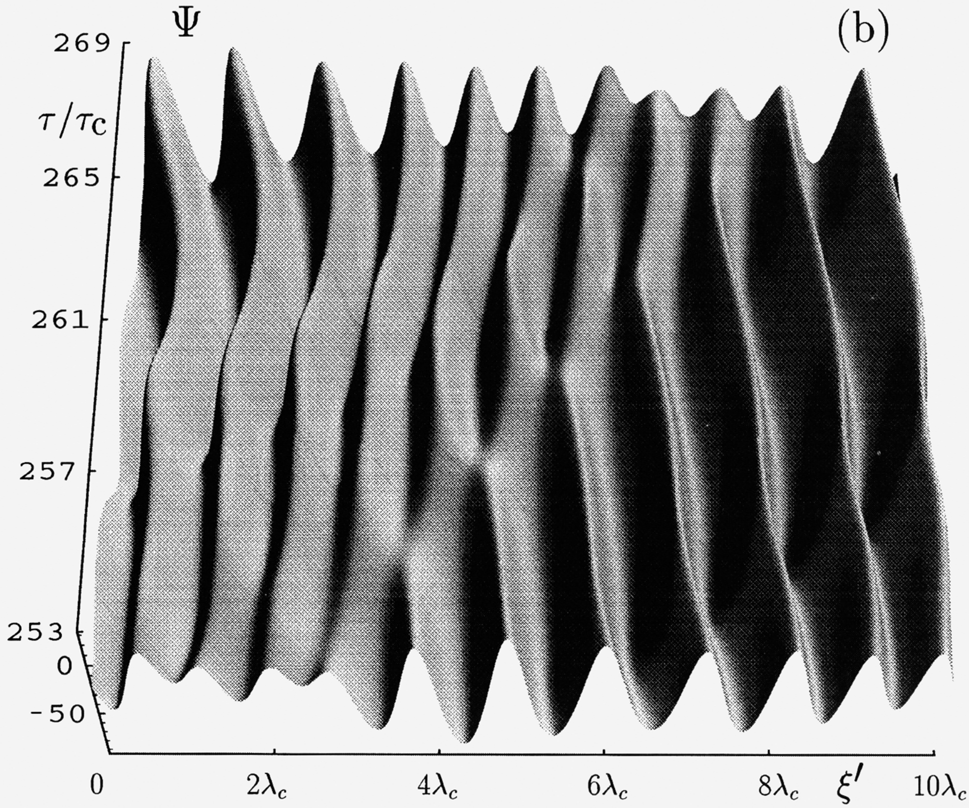

FIG. 2b. Numerical simulation of Eq. (3.9). $\langle\Psi\rangle$ versus time τ and $\xi' = \xi - v(\gamma)\tau$ for various values of γ ($0 < \xi' < 10\lambda_c$). $\gamma_1 = 1.33\gamma_c$, $v(\gamma_1) = 177.5$, $253 < \tau/\tau_c < 269$, $\tau_c = 2\pi\omega^{-1}(\gamma_2, k_c) = 0.253$.

resolution 512, while the control runs were conducted at the resolution 1024. The calculations were performed on an ALPHA-DEC workstation. As initial data in all simulations, the random fields were used. The problem was solved for three cases: $\gamma_1 = 1.1\gamma_c$, slightly above the stability threshold; $\gamma_2 = 1.33\gamma_c$, close to γ_c; $\gamma_3 = 5\gamma_c$, significantly above γ_c.

The spatio-temporal evolution of the flame interface Ψ is plotted in Figs. 2a, 2b, and 2c.

At $\gamma = \gamma_1$ the function Ψ appears to be nearly periodic both in ξ and τ. At $\gamma = \gamma_2$ the regular pattern disappears and at $\gamma = \gamma_3$ the interface dynamics assumes a clearly expressed chaotic behaviour. Yet, the solution still preserves the typical length-scale λ_c provided by the linear theory.

With the passage from γ_1 to γ_3 the spatial average $\langle\Psi\rangle$ markedly decreases. As a result the emerging corrugated structure undergoes a permanent drift along the ξ-axis stemming from the terms $2\Psi\Psi_\xi$ and $20\Psi_{\xi\xi\xi}$ of Eq. (3.9). For the sake of better visualization the interface evolution is shown in a moving frame $\xi' = \xi - V(\gamma)\tau$ with $V(\gamma) \cong 20k_c^2 - 2\langle\Psi\rangle$.

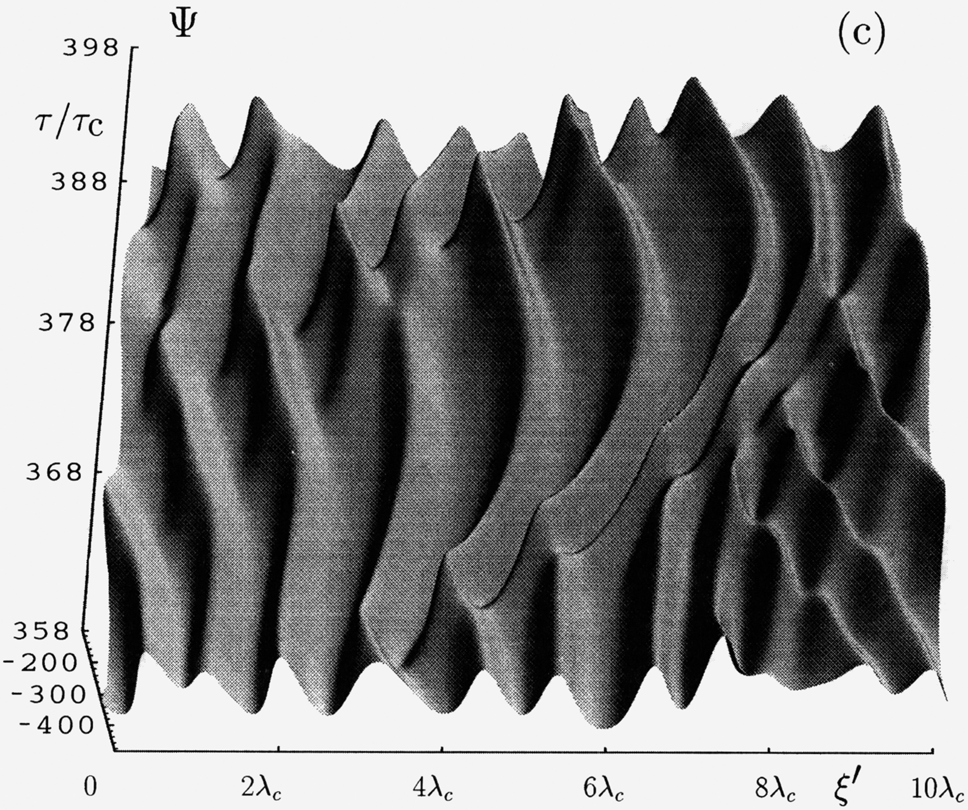

FIG. 2c. Numerical simulation of Eq. (3.9). $\langle\Psi\rangle$ versus time τ and $\xi' = \xi - v(\gamma)\tau$ for various values of γ $(0 < \xi' < 10\lambda_c)$. $\gamma_1 = 5\gamma_c$, $v(\gamma_1) = 746.4$, $358 < \tau/\tau_c < 398$, $\tau_c = 2\pi\omega^{-1}(\gamma_3, k_c) = 0.0785$.

5. Concluding remarks. The results obtained show that apart from small-scale high-intensity eddies certain slowly-varying fields may also affect the relaxational features of the large-scale flames. It is curious that the found shift in the effective dissipation rate cannot be captured within the framework of the stretch-based geometrical model (e.g., Williams, 1985):

$$F_t + \mathbf{v} \cdot \nabla F = v_F |\nabla F|, \tag{5.1}$$

$$v_F = 1 + (1 - \alpha)(\operatorname{div} \mathbf{n} + \mathbf{n} \cdot \nabla \mathbf{v} \cdot \mathbf{n}) \tag{5.2}$$

actively employed in studying various aspects of flame-flow interaction.[4] The reason for such an outcome is that the model (5.1)–(5.2) being valid for slowly-varying hydrodynamic fields and flames simply does not sense certain large-scale interaction, whose detection requires higher-order accuracy, not provided by the model.

[4]Equations (5.1)–(5.2) are written in nondimensional form employing the same set of units as the reaction-diffusion model of Sec. 2. $F(x, y, z, t) = 0$ is the flame interface and $\mathbf{n} = -\nabla F/|\nabla F|$ is its normal vector; v_F is the flame speed relative to the prescribed flow-field $\mathbf{v}$; v_F depends both on curvature of the flame and on $\mathbf{v}$.

Acknowledgments. These studies have been supported by the U. S. Department of Energy (Grant No. DE-FG02-88ER13822), by the National Science Foundation (Grant CTS-92-13414), by the U. S.-Israel Binational Science Foundation (Grant 93-00030), and by the Foundation for Basic Research of Tel-Aviv University.

Appendix A. Formal derivation of Equation (3.8). To conduct the necessary asymptotic expansions it is technically advantageous to perform the following change of spatial variables:

$$\varphi = \theta + at, \quad r = z + \Phi(\theta, t), \tag{A.1}$$

which eliminates the drift-induced time scale and fixes the location of the reaction zone at $z = 0$. In the new coordinates (θ, z, t) the set of original equations (2.1)–(2.2) becomes

$$D(\Theta) = L(\Theta), \qquad D(S) = L(S - \alpha\Theta) \tag{A.2}$$

where

$$D = \frac{\partial}{\partial t} + \left[a\Phi_\theta - \Phi_t + \frac{R}{z+\Phi} - \frac{aR^2\Phi_\theta}{(z+\Phi)^2}\right]\frac{\partial}{\partial z} + \left[\frac{aR^2}{(z+\Phi)^2} - a\right]\frac{\partial}{\partial\theta}, \tag{A.3}$$

$$L = \left[1 + \frac{\Phi_\theta}{(z+\Phi)^2}\right]\frac{\partial^2}{\partial z^2} + \left[\frac{1}{z+\Phi} - \frac{\Phi_{\theta\theta}}{(z+\Phi)^2}\right]\frac{\partial}{\partial z} + \frac{1}{(z+\Phi)^2}\frac{\partial^2}{\partial\theta^2} - \frac{2\Phi_\theta}{(z+\Phi)^2}\frac{\partial^2}{\partial z\partial\theta}. \tag{A.4}$$

The matching conditions (2.4)–(2.6) at the flame interface $z = 0$ become

$$[\Theta] = [S] = 0, \qquad \left(\sqrt{1 + \Phi_\theta^2/\Phi^2}\right)[\Theta_z] + \exp S = 0, \qquad [S_z - \alpha\Theta_z] = 0. \tag{A.5}$$

In the burnt gas region

$$\Theta = 1 \text{ at } z > 0 \quad \text{and} \quad S_z \text{ is bounded at } z \to \infty. \tag{A.6}$$

At the burner wall where $z = R_0 - \Phi(\theta, t)$, the boundary condition (2.8) yields

$$\Theta_z = R\Theta/R_0, \qquad S_z - \alpha\Theta_z = aR^2S/R_0. \tag{A.7}$$

The basic solution (2.9)–(2.10) corresponding to the undisturbed flame becomes

$$\Theta^b(z < 0) = (1 + (z/R))^R, \qquad S^b(z < 0) = \alpha R(1 + (z/R))^R \ln(1 + (z/R)). \tag{A.8}$$

As the next step one should pass to the scaled quantities as defined by the relations (3.1), (3.2), (3.4), (3.7). In the scaled variables and parameters the problem (A.2)–(A.7) may be written as

$$\begin{aligned} &- \varepsilon^3\overline{\Phi}_{\bar{t}}\Theta_z^b + \varepsilon^2\overline{\Theta}_z - \varepsilon^3\overline{\Phi}\,\overline{R}^{-1}\Theta_z^b - 2\varepsilon^3\bar{a}\overline{R}^{-1}z\overline{\Theta}_{\bar{\theta}} + 2\varepsilon^2\bar{a}\overline{R}^{-1}z\overline{\Phi}_{\bar{\theta}}\Theta_z^b \\ &\qquad + 2\varepsilon^3\bar{a}\overline{R}^{-1}\overline{\Phi}\,\overline{\Phi}_{\bar{\theta}}\Theta_z^b + \Theta_z^b - \varepsilon^2 z\Theta_z^b \\ &\quad = \Theta_{zz}^b + \varepsilon^2\overline{R}^{-1}\Theta_z^b + \varepsilon^2\overline{\Theta}_{zz} + \varepsilon^3\overline{R}^{-2}\overline{\Theta}_{\bar{\theta}\bar{\theta}} - \varepsilon^2\overline{R}^{-2}\overline{\Phi}_{\bar{\theta}\bar{\theta}}^2\Theta_z^b + \varepsilon^3\overline{R}^{-2}\overline{\Phi}_{\bar{\theta}}^2\Theta_{zz}^b + O(\varepsilon^4), \end{aligned} \tag{A.9}$$

$$
\begin{aligned}
&- \varepsilon^3\overline{\Phi}_{\bar t}S^b_z + \varepsilon^2\overline{S}_z - \varepsilon^3\overline{\Phi}\,\overline{R}^{-1}S^b_z - 2\varepsilon^3\bar a\overline{R}^{-1}z\overline{S}_{\bar\theta} + 2\varepsilon^2\bar a\overline{R}^{-1}z\overline{\Phi}_{\bar\theta}S^b_z \\
&\quad + 2\varepsilon^3\bar a\overline{R}^{-1}\overline{\Phi}\,\overline{\Phi}_{\bar\theta}S^b_z + S^b_z - \varepsilon^2 zS^b_z \\
&\quad = (S^b-\alpha\Theta^b)_{zz} + \varepsilon^2\overline{R}^{-1}(S^b-\alpha\Theta^b)_z + \varepsilon^2(\overline{S}-\alpha\overline{\Theta})_{zz} + \varepsilon^3\overline{R}^{-2}(\overline{S}-\alpha\overline{\Theta})_{\bar\theta\bar\theta} \\
&\quad - \varepsilon^2\overline{R}^{-2}\overline{\Phi}_{\bar\theta\bar\theta}(S^b-\alpha\Theta^b)_z + \varepsilon^3\overline{R}^{-2}\overline{\Phi}^2_{\bar\theta}(S^b-\alpha\Theta^b)_{zz} + O(\varepsilon^4),
\end{aligned}
\tag{A.10}
$$

$$
[\overline{\Theta}] = [\overline{S}] = 0, \quad [\overline{S}_z - \alpha\overline{\Theta}] = 0, \quad [\overline{\Theta}_z] + \overline{S} - \tfrac{1}{2}\varepsilon\overline{R}^{-2}(\overline{\Phi}_{\bar\theta})^2 + O(\varepsilon^2) = 0 \text{ at } z = 0,
\tag{A.11}
$$

$$
\overline{\Theta} \to 0,\ \overline{S} \to 0 \text{ at } z \to -\infty.
\tag{A.12}
$$

$$
\overline{\Theta} = 0 \text{ for } z > 0 \text{ and } \overline{S} \text{ grows not faster than an integer power of } z \text{ at } z \to +\infty.
\tag{A.13}
$$

The last requirement ensures the compatibility with the boundary condition (A.6) which, unlike (A.7), is achieved not at $z = O(1)$ but rather at $z = O(1/\varepsilon)$. Note that the basic solution Θ^b, S^b is ε-dependent both through $R = \varepsilon^{-2}\overline{R}$ and $\alpha = 1 + \varepsilon$:

$$
\Theta^b = \Theta^b_0 + O(\varepsilon^2) \text{ where } \Theta^b_0\ (z<0) = \exp z \quad\text{and}\quad \Theta^b_0\ (z>0) = 1,
\tag{A.14}
$$

$$
S^b = S^b_0 + \varepsilon S^b_1 + O(\varepsilon^2),
$$

where

$$
S^b_0\ (z<0) = S^b_1\ (z<0) = z\exp z,
$$

and

$$
S^b_0\ (z>0) = S^b_1\ (z>0) = 0.
\tag{A.15}
$$

The unknown functions $\overline{\Phi}$, $\overline{\Theta}$, and $\overline{S}$ are sought as asymptotic expansions in integer powers of ε:

$$
\overline{\Phi} = \overline{\Phi}^0 + \varepsilon\overline{\Phi}^1 + O(\varepsilon^2), \quad \overline{\Theta} = \overline{\Theta}^0 + \varepsilon\overline{\Theta}^1 + O(\varepsilon^2), \quad \overline{S} = \overline{S}^0 + \varepsilon\overline{S}^1 + O(\varepsilon^2).
\tag{A.16}
$$

For the zeroth approximation the system (A.10)–(A.13) yields

$$
\overline{\Theta}^0_z - \overline{\Theta}^0_{zz} = -2\bar a\overline{R}^{-1}z\overline{\Phi}^0_{\bar\theta}\Theta^b_{0z} - \overline{R}^{-2}\overline{\Phi}^0_{\bar\theta\bar\theta}\Theta^b_{0z},
\tag{A.17}
$$

$$
\overline{S}^0_z - \overline{S}^0_{zz} + \overline{\Theta}^0_{zz} = -2\bar a\overline{R}^{-1}z\overline{\Phi}^0_{\bar\theta}S^b_{0z} - \overline{R}^{-2}\overline{\Phi}^0_{\bar\theta\bar\theta}S^b_{0z} + \overline{R}^{-2}\overline{\Phi}^0_{\bar\theta\bar\theta}\Theta^b_{0z},
\tag{A.18}
$$

$$
[\overline{\Theta}^0] = [\overline{S}^0] = 0, \quad [\overline{\Theta}^0_z] - [\overline{S}^0_z] = 0, \quad [\overline{\Theta}^0_z] + \overline{S}^0 = 0 \text{ at } z = 0,
\tag{A.19}
$$

$$
\overline{\Theta}^0 \to 0,\ \overline{S}^0 \to 0 \quad \text{at } z \to -\infty,
\tag{A.20}
$$

$$
\overline{\Theta}^0 = 0 \text{ at } z > 0 \quad\text{and}\quad \overline{S}^0_z < \infty \text{ at } z \to +\infty.
\tag{A.21}
$$

Hence, one obtains $\overline{\Theta}^0$, $\overline{S}^0$ expressed in terms of $\overline{\Phi}^0$ (still unknown at this stage). The solution of the problem (A.17)–(A.18) is of the form

$$\begin{aligned} &\overline{\Theta}^0(z<0) = (\overline{R}^{-2}\overline{\Phi}^0_{\bar\theta\bar\theta} - 2\bar a\overline{R}^{-1}\overline{\Phi}^0_{\bar\theta})z\exp z + \bar a\overline{R}^{-1}\overline{\Phi}^0_{\bar\theta}z^2\exp z,\\ &\overline{\Theta}^0(z>0) = 0, \end{aligned} \tag{A.22}$$

$$\begin{aligned} \overline{S}^0(z<0) &= (\overline{R}^{-2}\overline{\Phi}^0_{\bar\theta\bar\theta} - 2\bar a\overline{R}^{-1}\overline{\Phi}^0_{\bar\theta})\exp z + (\overline{R}^{-2}\overline{\Phi}^0_{\bar\theta\bar\theta} - \bar a\overline{R}^{-1}\overline{\Phi}^0_{\bar\theta})z^2\exp z\\ &\quad + \bar a\overline{R}^{-1}\overline{\Phi}^0_{\bar\theta}z^3\exp z,\\ \overline{S}^0(z>0) &= \overline{R}^{-2}\overline{\Phi}^0_{\bar\theta\bar\theta} - 2\bar a\overline{R}^{-1}\overline{\Phi}^0_{\bar\theta}. \end{aligned} \tag{A.23}$$

For the first approximation the system (A.10)–(A.13) gives

$$\begin{aligned} \overline{\Theta}^1_z - \overline{\Theta}^1_{zz} &= \overline{\Phi}^0_{\bar t}\Theta^b_{0z} + \overline{\Phi}^0\overline{R}^{-1}\Theta^b_{0z} + 2\bar a\overline{R}^{-1}z\overline{\Theta}^0_{\bar\theta} - 2\bar a\overline{R}^{-1}z\overline{\Phi}^1_{\bar\theta}\Theta^b_{0z}\\ &\quad - 2\bar a\overline{R}^{-1}\overline{\Phi}^0\overline{\Phi}^0_{\bar\theta}\Theta^b_{0z} + \overline{R}^{-2}\overline{\Theta}^0_{\bar\theta\bar\theta} - \overline{\Phi}^1_{\bar\theta\bar\theta} - \overline{R}^{-2}\Theta^b_{0z} + \overline{R}^{-2}(\overline{\Phi}^0_{\bar\theta})^2\Theta^b_{0zz}, \end{aligned} \tag{A.24}$$

$$\begin{aligned} \overline{S}^1_z - \overline{S}^1_{zz} + \overline{\Theta}^1_{zz} + \overline{\Theta}^0_{zz} &= \overline{\Phi}^0_{\bar t}S^b_{0z} + \overline{\Phi}^0\overline{R}^{-1}S^b_{0z} + 2\bar a\overline{R}^{-1}z\overline{S}^0_{\bar\theta} - 2\bar a\overline{R}^{-1}z\overline{\Phi}^1_{\bar\theta}(S^b_0 + S^b_1)_z\\ &\quad - 2\bar a\overline{R}^{-1}\overline{\Phi}^0\overline{\Phi}^0_{\bar\theta}S^b_{0z} + \overline{R}^{-2}(\overline{S}^0 - \overline{\Theta}^0)_{\bar\theta\bar\theta} - \overline{\Phi}^1_{\bar\theta\bar\theta}\overline{R}^{-2}(S^b_0 - \Theta^b_0)_z\\ &\quad - \overline{\Phi}^0_{\bar\theta\bar\theta}\overline{R}^{-2}(S^b_1 - \Theta^b_0)_z + \overline{R}^{-2}(\overline{\Phi}^0_{\bar\theta})^2(S^b_0 - \Theta^b_0)_{zz}, \end{aligned} \tag{A.25}$$

$$[\overline{\Theta}^1] = [\overline{S}^1] = 0 \quad \text{at } z=0, \tag{A.26}$$

$$[\overline{\Theta}^1_z] + \overline{S}^1 = \tfrac{1}{2}\overline{R}^{-2}(\overline{\Phi}^0_{\bar\theta})^2 \quad \text{at } z=0, \tag{A.27}$$

$$[\overline{\Theta}^1_z - \overline{S}^1_z] = -[\overline{\Theta}^0_z] \quad \text{at } z=0, \tag{A.28}$$

$$\overline{\Theta}^1 \to 0,\ \overline{S}^1 \to 0 \quad \text{at } z\to-\infty, \tag{A.29}$$

$$\overline{\Theta}^1 = 0 \text{ at } z>0 \quad \text{and} \quad \overline{S}^1_{zz} < \infty \text{ at } z\to+\infty. \tag{A.30}$$

Solution of the system (A.24), (A.25) meeting the conditions (A.26), (A.29), (A.30) and thereby apart from $\overline{\Phi}^0$, $\overline{\Phi}^1$ involving also $\overline{S}^1(0)$ reads

$$\begin{aligned} \overline{\Theta}^1(z<0) &= (-\overline{\Phi}^0_{\bar t} + \overline{R}^{-4}\overline{\Phi}^0_{\bar\theta\bar\theta\bar\theta\bar\theta} - 8\bar a\overline{R}^{-3}\overline{\Phi}^0_{\bar\theta\bar\theta\theta} - \overline{R}^{-2}(\overline{\Phi}^0_{\bar\theta})^2\\ &\quad + 20\bar a^2\overline{R}^{-2}\overline{\Phi}^0_{\bar\theta\bar\theta} + \overline{R}^{-2}\overline{\Phi}^1_{\bar\theta\bar\theta} - \overline{R}^{-1}\overline{\Phi}^0 + 2\bar a\overline{R}^{-1}\overline{\Phi}^0\overline{\Phi}^0_{\bar\theta} - 2\bar a\overline{R}^{-1}\overline{\Phi}^1_{\bar\theta})z\exp z\\ &\quad + (-\tfrac{1}{2}\overline{R}^{-4}\overline{\Phi}^0_{\bar\theta\bar\theta\bar\theta\bar\theta} + 4\bar a\overline{R}^{-3}\overline{\Phi}^0_{\bar\theta\bar\theta\bar\theta} - 10\bar a^2\overline{R}^{-2}\overline{\Phi}^0_{\bar\theta\bar\theta} + \bar a\overline{R}^{-1}\overline{\Phi}^1_{\bar\theta})z^2\exp z\\ &\quad + (-\bar a\overline{R}^{-3}\overline{\Phi}^0_{\bar\theta\bar\theta\bar\theta} + \tfrac{10}{3}\bar a^2\overline{R}^{-2}\overline{\Phi}^0_{\bar\theta\bar\theta})z^3\exp z - \tfrac{1}{2}\bar a^2\overline{R}^{-2}\overline{\Phi}^0_{\bar\theta\bar\theta}z^4\exp z,\\ \overline{\Theta}^1(z<0) &= 0, \end{aligned} \tag{A.31}$$

$$
\begin{aligned}
\overline{S}^1(z<0) = {} & \overline{S}^1(0)\exp z + (-\overline{\Phi}^0_{\bar t} - 3\overline{R}^{-4}\overline{\Phi}^0_{\bar\theta\bar\theta\bar\theta\bar\theta} + 20\bar a\overline{R}^{-3}\overline{\Phi}^0_{\bar\theta\bar\theta\bar\theta} - \overline{R}^{-2}(\overline{\Phi}^0_{\bar\theta})^2 \\
& - 44\bar a^2\overline{R}^{-2}\overline{\Phi}^0_{\bar\theta\bar\theta} - \overline{R}^{-1}\overline{\Phi}^0 + 2\bar a\overline{R}^{-1}\overline{\Phi}^0\overline{\Phi}^0_{\bar\theta})z\exp z + (-\overline{\Phi}^0_{\bar t} + \tfrac{3}{2}\overline{R}^{-4}\overline{\Phi}^0_{\bar\theta\bar\theta\bar\theta\bar\theta} \\
& - 13\bar a\overline{R}^{-3}\overline{\Phi}^0_{\bar\theta\bar\theta\bar\theta} - \overline{R}^{-2}(\overline{\Phi}^0_{\bar\theta})^2 + \overline{R}^{-2}\overline{\Phi}^0_{\bar\theta\bar\theta} + 32\bar a^2\overline{R}^{-2}\overline{\Phi}^0_{\bar\theta\bar\theta} + \overline{R}^{-2}\overline{\Phi}^1_{\bar\theta\bar\theta} - \overline{R}^{-1}\overline{\Phi}^0 \\
& - \bar a\overline{R}^{-1}\overline{\Phi}^0_{\bar\theta} + 2\bar a\overline{R}^{-1}\overline{\Phi}^0\overline{\Phi}^0_{\bar\theta} - \bar a\overline{R}^{-1}\overline{\Phi}^1_{\bar\theta})z^2\exp z + (-\tfrac{1}{2}\overline{R}^{-4}\overline{\Phi}^0_{\bar\theta\bar\theta\bar\theta\bar\theta} + 4\bar a\overline{R}^{-3}\overline{\Phi}^0_{\bar\theta\bar\theta\bar\theta} \\
& - 10\bar a^2\overline{R}^{-2}\overline{\Phi}^0_{\bar\theta\bar\theta} + \bar a\overline{R}^{-1}\overline{\Phi}^0_{\bar\theta} + \bar a\overline{R}^{-1}\overline{\Phi}^1_{\bar\theta})z^3\exp z + (-\bar a\overline{R}^{-3}\overline{\Phi}^0_{\bar\theta\bar\theta\bar\theta} \\
& + \tfrac{17}{6}\bar a^2\overline{R}^{-2}\overline{\Phi}^0_{\bar\theta\bar\theta})z^4\exp z - \tfrac{1}{2}\bar a^2\overline{R}^{-2}\overline{\Phi}^0_{\bar\theta\bar\theta}z^5\exp z, \\
\overline{S}^1(z>0) = {} & \overline{S}^1(0) + (\overline{R}^{-4}\overline{\Phi}^0_{\bar\theta\bar\theta\bar\theta\bar\theta} - 4\bar a^2\overline{R}^{-2}\overline{\Phi}^0_{\bar\theta\bar\theta})z + (\bar a\overline{R}^{-3}\overline{\Phi}^0_{\bar\theta\bar\theta\bar\theta} - 2\bar a^2\overline{R}^{-2}\overline{\Phi}^0_{\bar\theta\bar\theta})z^2.
\end{aligned}
\tag{A.32}
$$

The remaining boundary conditions (A.27), (A.28) imply

$$
\begin{aligned}
\overline{R}^{-2}\overline{\Phi}^1_{\bar\theta\bar\theta} - 2\bar a\overline{R}^{-1}\overline{\Phi}^1_{\bar\theta} - \overline{S}^1(0) = {} & \overline{\Phi}^0_{\bar t} + \overline{R}^{-1}\overline{\Phi}^0 - 20\bar a\overline{R}^{-2}\overline{\Phi}^0_{\bar\theta\bar\theta} + 8\bar a\overline{R}^{-3}\overline{\Phi}^0_{\bar\theta\bar\theta\bar\theta} \\
& - \overline{R}^{-4}\overline{\Phi}^0_{\bar\theta\bar\theta\bar\theta\bar\theta} - 2\bar a\overline{R}^{-1}\overline{\Phi}^0\overline{\Phi}^0_{\bar\theta} + \tfrac{1}{2}\overline{R}^{-2}(\overline{\Phi}^0_{\bar\theta})^2,
\end{aligned}
\tag{A.33}
$$

$$
\begin{aligned}
& \overline{R}^{-2}\overline{\Phi}^1_{\bar\theta\bar\theta} - 2\bar a\overline{R}^{-1}\overline{\Phi}^1_{\bar\theta} - \overline{S}^1(0) \\
& \quad = -2\bar a\overline{R}^{-1}\overline{\Phi}^0_{\bar\theta} + \overline{R}^{-2}(1+60\bar a^2)\overline{\Phi}^0_{\bar\theta\bar\theta} - 28\bar a\overline{R}^{-3}\overline{\Phi}^0_{\bar\theta\bar\theta\bar\theta} + 5\overline{R}^{-4}\overline{\Phi}^0_{\bar\theta\bar\theta\bar\theta\bar\theta}.
\end{aligned}
\tag{A.34}
$$

Since the r.h.s. of the relations obtained are identical, they are compatible only provided that their l.h.s. are identical as well. Hence, one ends up with the sought-for equation for the interface $\overline{\Phi}^0$:

$$
\begin{aligned}
\overline{\Phi}^0_{\bar t} - 2\bar a\overline{R}^{-1}\overline{\Phi}^0_{\bar\theta} + \tfrac{1}{2}\overline{R}^{-2}(\overline{\Phi}^0_{\bar\theta})^2 - 2\bar a\overline{R}^{-1}\overline{\Phi}^0\overline{\Phi}^0_{\bar\theta} + \overline{R}^{-2}(1+40\bar a^2)\overline{\Phi}^0_{\bar\theta\bar\theta} \\
- 20\bar a\overline{R}^{-3}\overline{\Phi}^0_{\bar\theta\bar\theta\bar\theta} + 4\overline{R}^{-4}\overline{\Phi}^0_{\bar\theta\bar\theta\bar\theta\bar\theta} + \overline{R}^{-1}\overline{\Phi}^0 = 0.
\end{aligned}
\tag{A.35}
$$

By a shift transformation $\bar\theta + 2\bar a\overline{R}^{-1}\bar t \to \bar\theta$ one eliminates the drift term $-2\bar a\overline{R}^{-1}\overline{\Phi}^0_{\bar\theta}$. Setting $\overline{R}\bar\theta = \bar x$ one finally arrives at Eq. (3.8).

References

[1] A. Bayliss and B. J. Matkowsky, *Two routes to chaos in condensed phase combustion*, SIAM J. Appl. Math. **50**, 437–459 (1990)

[2] B. J. Matkowsky and G. I. Sivashinsky, *An asymptotic derivation of two models in flame theory associated with the constant density approximation*, SIAM J. Appl. Math. **37**, 686–699 (1979)

[3] D. M. Michelson and G. I. Sivashinsky, *On irregular wavy flow of a liquid film down a vertical plane*, Prog. Theor. Phys. **63**, 2112–2114 (1980)

[4] G. I. Sivashinsky, *On self-turbulization of a laminar flame*, Acta Astronautica **6**, 569–591 (1979)

[5] G. I. Sivashinsky, *On the intrinsic dynamics of premixed flames*, Proc. Roy. Soc. London **A332**, 135–148 (1990)

[6] G. I. Taylor, *Dispersion of soluble matter in solvent flowing slowly through a tube*, Proc. Roy. Soc. London **A219**, No. 1137, 186–203 (1953)

[7] F. A. Williams, *Combustion Theory*, The Benjamin/Cummings Publishing Co., New York, 1985